Fluorescent Surfactants from Common Dyes – Rhodamine B and Eosin Y

Ashleigh D. Smith McWilliams[1], Selin Ergülen[1], Meredith M. Ogle[1], Carlos A. de los Reyes[1], Matteo Pasquali[1,2,3,5], and Angel A. Martí[1,3,4,5,*]

[1] Department of Chemistry, Rice University, Houston, Texas 77005, USA. [2]Department of Chemical and Biomolecular Engineering, Rice University, Houston, Texas 77005, USA. [3]Deparment of Materials Science and Nanoengineering, Rice University, Houston, Texas 77005, USA. [4]Department of Bioengineering, Rice University, Houston, Texas 77005, USA. [5]Smalley-Curl Institute for Nanoscale Science and Technology, Rice University, Houston, Texas 77005, USA. *Email: amarti@rice.edu

1 Abstract

Eight fluorescent surfactants were synthesized by attaching aliphatic chains of 6, 10, 12, or 16 carbons to the fluorescent dyes Rhodamine B and Eosin Y. The obtained critical micelle concentrations (CMC) demonstrate an increasing CMC with decreasing aliphatic chain length, which is a typical behavior for surfactants. Additionally, fluorescence quantum yield experiments show a decrease in quantum yield with increasing aliphatic chain length, suggesting that the tails can interact with the dye, influencing its excited state. Finally, applications for the fluorescent surfactants were demonstrated; as a cellular stain in Panc-1 cells and as a dispersion and imaging tool for carbon and boron nitride nanotubes. These surfactants could provide a useful tool for a wide array of potential applications, from textile dyes to fluorescence imaging.

2 Introduction

Surfactants are commonly utilized molecules in a wide array of industries, from personal care products to fuel additives.[1,2] There are four classifications of surfactants, which are based on the molecule's charge – anionic, cationic, nonionic, or zwitterionic.[1,2] In all cases they are amphiphilic molecules, consisting of a hydrophilic group and a hydrophobic chain, where the hydrophobic tail prefers to avoid interaction with water molecules while the hydrophilic head seeks to increase its interactions with them. Once enough surfactant has been added to a solution, the hydrophobic effect will drive the formation of micelles, in which their hydrophobic chains are

protected from water by a shell composed of the hydrophilic heads. The concentration at which micelles begin to form is called the critical micelle concentration (CMC). This concentration is dependent on the surfactant's properties, particularly the length of the aliphatic chain.[1,3,4]

The unique properties of surfactants make them ideal for many different applications. Their use spans numerous industries, from food and personal care to petroleum and environmental remediation.[1,2,5,6] Perhaps the most well-known use of surfactants is as the primary agent in detergents and soaps; however, they are also commonly utilized in wetting agents, industrial foams, and drug-delivery, among others.[1,2] The vast applications of surfactants has spurred the continued study of new surfactant systems. One type of surfactant that has not been fully studied and developed is a fluorescent surfactant.

Adding fluorescence capabilities to the already unique properties of surfactants further expands the potential applications for these systems. In many applications, surfactants and dyes are both utilized to obtain a certain result. However, combining these two components into a single compound would reduce the steps and materials required and improve the efficiency of the process. For example, fluorescent or dye-based surfactants could be used in paint production,[7] fabric or textile dyeing,[8] and in fluorescence microscopy applications, such as imaging of materials[9-11] or targeted cell staining.[12] Current work in fluorescent surfactants has only scratched the surface of these possibilities.[13-16]

We propose a simple conjugation for the production of fluorescent surfactants that has the distinct benefits of a simple synthetic approach and impressive adaptability. Our surfactants are prepared through a mild esterification reaction between common fluorescent dyes, Rhodamine B and Eosin Y, and aliphatic alcohols of varied carbon chain lengths. Though some of these dye-ester structures have been previously reported, [17-22] in depth fluorescence characterization and CMC for the different surfactants is lacking from the literature. The simplicity of this approach makes it easily adaptable to a wide array of common dyes, allowing for a selection in desired wavelength and charge. Additionally, the length of the alcohol utilized will manipulate the surfactant properties to fit a particular application.

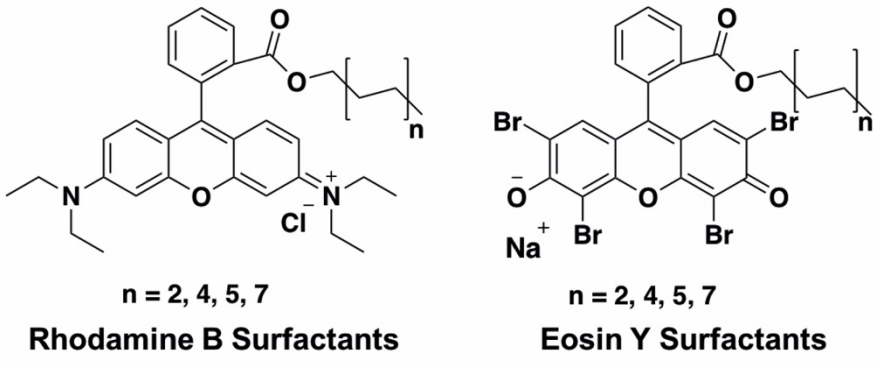

Fig. 1: Structures of fluorescent surfactants.

In this manuscript eight fluorescent surfactants (Fig. 1) were prepared by adding aliphatic chains of 6, 10, 12, and 16 carbons to two fluorescent dyes (Rhodamine B & Eosin Y). This was achieved through an esterification reaction between the carboxylic acid present on each dye and an alcohol with the desired aliphatic chain length. The chosen fluorescent dyes provide both anionic and cationic surfactants with different fluorescent properties for varied applications. Surfactants will be denoted based on the dye (R for Rhodamine and E for Eosin) and the aliphatic chain length (6, 10, 12, or 16). For example, a Rhodamine surfactant with an aliphatic chain length of 16 will be denoted as R16. Each surfactant was characterized by ^{1}H and ^{13}C NMR and the critical micelle concentration and fluorescent quantum yield were measured for each. Here we report the surfactants syntheses and analyses. We also demonstrate applications for the produced surfactants; as tools for fluorescence imaging of cells and nanomaterials, carbon and boron nitride nanotubes. We believe these fluorescence surfactants can be used to stain and label different structures ranging from cells, to nanostructures, to textiles.

3 Experimental Section

Materials. Rhodamine B was purchased from Acros and Eosin Y was obtained from Sigma-Aldrich. Alcohols were purchased from Aldrich (hexadecanol, dodecanol, & hexanol) and Acros (decanol). All chemicals were used as received with no further purification. Carbon nanotubes were HiPco SWCNTs obtained from NanoIntegris (lot HR32-009) and purified by a previously reported method.[23] Boron nitride nano-

tubes were Q1β type obtained from BNNT, LLC and purified by a reported methodology.[24]

General Procedure for Surfactant Synthesis. The surfactants were synthesized by a previously reported, mild esterification reaction based on the Garegg-Samuelsson reaction.[25] CH_2Cl_2 (~4 mL) was added to an oven-dried round-bottom flask equipped with a stir bar. I_2 (0.15 mmol), Ph_3P (0.15 mmol), imidazole (0.33 mmol), and either Rhodamine B or Eosin Y (0.1 mmol) were added to the flask while stirring. The solution was allowed to stir for 5 minutes before the alcohol (0.15 mmol) was added. Then the reaction was stirred for 24 hours in the dark. The crude product was washed with 2N HCl and water before being dried with $MgSO_4$ and the solvent removed under vacuum. The product was purified by column chromatography in a 1:1:1 mixture of DCM, hexanes, and acetone and characterized by NMR (see ESI for spectra).

R6: ^{1}H NMR (500 MHz, MeOD) δ 8.23 (dd, 1H, J=6.5Hz, 1Hz), 7.76 (dtd, 2H, J=9Hz, 6.5Hz, 1.5Hz), 7.37 (dd, 1H, J=6Hz, 1Hz), 7.07 (d, 2H, J=9.5Hz), 6.98 (dd, 2H, J=7Hz, 2.5Hz), 6.93 (d, 2H, 2.5Hz), 3.86 (t, 2H, J=6.5Hz), 3.62 (q, 8H, J=7.5Hz), 1.06 (m, 20H), 0.76 (t, 3H, J=7.5Hz). ^{13}C NMR (125 MHz, MeOD) δ 167.07, 160.28, 159.47, 157.31, 134.69, 134.13, 132.60, 132.48, 132.10, 131.75, 131.65, 115.70, 114.96, 97.43, 66.91, 46.99, 32.73, 29.67, 26.82, 23.66, 14.54, 12.97.

R10: ^{1}H NMR (500 MHz, MeOD) δ 8.23 (dd, 1H, J=6Hz, 1.5Hz), 7.76 (dtd, 2H, J=8Hz, 6Hz, 1.5Hz), 7.36 (dd, 1H, J=6Hz, 1Hz), 7.07 (d, 2H, J=10Hz), 6.98 (dd, 2H, J=7Hz, 2.5Hz), 6.92 (d, 2H, 2.5Hz), 3.86 (t, 2H, J=6.5Hz), 3.61 (q, 8H, J=7Hz), 1.15 (m, 27H), 0.82 (t, 3H, J=7.5Hz). ^{13}C NMR (125 MHz, MeOD) δ 167.08, 160.33, 159.49, 157.32, 134.71, 134.14, 132.62, 132.50, 132.11, 131.77, 131.67, 115.71, 114.99, 97.44, 66.91, 47.03, 33.22, 30.85, 30.68, 30.58, 30.47, 29.55, 27.11, 23.89, 14.60, 13.01.

R12: ^{1}H NMR (500 MHz, MeOD) δ 8.21 (dd, 1H, J=7Hz, 1Hz), 7.74 (dtd, 2H, J=9Hz, 6Hz, 1.5Hz), 7.34 (dd, 1H, J=6.5Hz, 1Hz), 7.05 (d, 2H, J=9.5Hz), 6.96 (dd, 2H, J=9.5Hz, 2.5Hz), 6.91 (d, 2H, 2.5Hz), 3.84 (t, 2H, J=6.5Hz), 3.59 (q, 8H, J=7Hz), 1.18 (m, 32H), 0.80 (t, 3H, J=7Hz). ^{13}C NMR (125 MHz, MeOD) δ 167.08, 160.33, 159.49, 157.31, 134.71, 134.16, 132.63, 132.51, 132.10, 131.78, 131.68, 115.71, 114.99, 97.44, 66.92, 47.03, 33.23, 30.93, 30.91, 30.89, 30.69, 30.65, 30.48, 29.56, 27.12, 23.90, 14.61, 13.01.

R16: ^{1}H NMR (500 MHz, MeOD) δ 8.21 (dd, 1H, J=6.5Hz, 1Hz), 7.74 (dtd, 2H, J=8.5Hz, 6Hz, 1.5Hz), 7.34 (dd, 1H, J=6Hz, 1Hz), 7.05 (d, 2H, J=9.5Hz), 6.96 (dd, 2H, J=7Hz, 2.5Hz), 6.90 (d, 2H, 2.5Hz), 3.84 (t, 2H, J=6Hz), 3.59 (q, 8H, J=7Hz), 1.21 (m, 41H), 0.80 (t, 3H, J=5Hz). ^{13}C NMR (125 MHz, MeOD) δ 167.49, 160.37, 159.51, 157.34, 134.71, 134.14, 132.64, 132.51, 132.13, 131.77, 131.68, 115.71,

115.00, 97.44, 66.92, 47.02, 33.23, 30.93, 30.91, 30.88, 30.87, 30.86, 30.66, 30.63, 30.47, 29.56, 27.11, 23.89, 14.59, 13.00.

E6: ^{1}H NMR (500 MHz, DMSO-d6) δ 8.21 (dd, 1H, J=6.5Hz, 1.5Hz), 7.86 (dtd, 2H, J=18.5Hz, 6Hz, 1Hz), 7.56 (dd, 1H, J=7Hz, 0.5Hz), 7.02 (s, 2H), 3.92 (t, 2H, J=6Hz), 1.00 (m, 11H). ^{13}C NMR (125 MHz, DMSO-d6) δ 168.54, 152.93, 131.77, 131.48, 130.67, 130.10, 129.56, 129.31, 118.50, 109.18, 99.71, 76.54, 65.36, 55.29, 30.06, 29.75, 29.58, 25.16, 21.56, 13.95.

E10: ^{1}H NMR (500 MHz, DMSO-d6) δ 8.21 (dd, 1H, J=7Hz, 1Hz), 7.88 (dtd, 2H, J=19Hz, 6Hz, 1.5Hz), 7.55 (dd, 1H, J=7Hz, 0.5Hz), 6.99 (s, 2H), 3.92 (t, 2H, J=6Hz), 1.05 (m, 19H). ^{13}C NMR (125 MHz, DMSO-d6) δ 168.30, 152.93, 132.98, 130.60, 130.31, 130.06, 129.75, 129.01, 118.51, 109.18, 99.52, 76.54, 65.22, 55.29, 31.29, 28.98, 28.75, 28.67, 28.64, 28.60, 27.82, 25.42, 22.09, 13.97.

E12: ^{1}H NMR (500 MHz, DMSO-d6) δ 8.14 (dd, 1H, J=7Hz, 1Hz), 7.81 (dtd, 2H, J=19Hz, 6.5Hz, 1Hz), 7.49 (dd, 1H, J=6.5Hz, 1Hz), 6.93 (s, 2H), 3.92 (t, 2H, J=6Hz), 1.03 (m, 23H). ^{13}C NMR (125 MHz, DMSO-d6) δ 168.30, 152.92, 132.86, 130.65, 130.60, 130.07, 129.08, 129.01, 118.50, 109.18, 99.52, 72.31, 65.29, 55.29, 31.29, 29.00, 28.97, 28.94, 28.73, 28.70, 28.67, 28.63, 27.81, 25.42, 22.09, 13.96.

E16: ^{1}H NMR (500 MHz, DMSO-d6) δ 8.14 (dd, 1H, J=7Hz, 1Hz), 7.81 (dtd, 2H, J=19Hz, 6.5Hz, 1.5Hz), 7.49 (dd, 1H, J=6.5Hz, 1Hz), 6.93 (s, 2H), 3.91 (t, 2H, J=6Hz), 1.09 (m, 31H). ^{13}C NMR (125 MHz, DMSO-d6) δ 168.38, 153.11, 133.14, 130.69, 130.33, 130.07, 129.77, 129.02, 118.52, 109.19, 99.54, 76.78, 65.23, 55.69, 31.28, 29.75, 29.72, 29.70, 29.05, 29.00, 28.90, 28.70, 28.63, 25.42, 22.08, 13.94.

Critical micelle concentration measurements. The critical micelle concentration of each surfactant was determined by measuring interfacial tension as a function of surfactant concentration. The pendant drop method[26] was utilized for interfacial tension measurements. Each pendant drop was produced with ca. 5 μL of surfactant solution and recorded using a Ramé-hart contact angle goniometer (Model 100-01S) with a U1 series super speed digital camera and DROPimage Standard software. The pendant drops were analyzed using an ImageJ Plugin.[27] Rhodamine surfactants were first dissolved in methanol and then diluted to their final concentration in water. The methanol concentration was < 5% for all measurements.

Spectroscopic studies. Absorbance measurements were acquired using a Shimadzu 2450 UV-Visible spectrophotometer. Photoluminescence spectra were measured with a Horiba Nanolog Spectrophotometer. All samples were excited at 485 nm and recorded from 500 to 720 nm. Quantum yield (ϕ) measurements were performed using Rhodamine B as a standard (ϕ_{ST} = 0.31).[28] All samples were prepared by dissolving

the compound in methanol and diluting with water until the desired absorbance at 485 nm was reached. The methanol concentration was < 1% for all measurements.

Cell staining. Panc-1 cells were maintained with Dulbecco Modified Eagle Medium with 10% fetal bovine serum and 1% penicillin and streptomycin at 37 °C and 5% CO_2. Cells were plated onto microscope slides at 30,000 cell/mL and adhered for 6h. Cells were rinsed with PBS and fixed with paraformaldehyde (4% in PBS) at room temperature for 20 min. After another rinse with PBS, cells were stained with the R16 surfactant (500 nM in PBS) and incubated at room temperature for 20 min. Cells were rinsed and mounted with ProLong AntiFade Gold with DAPI. Images were taken on a Nikon A1R confocal microscope using 40x and 60x oil immersion objectives (compressed z-stack: 60x oil immersion objective) with DAPI and TRITC channels.

Nanomaterial imaging. Carbon nanotubes (CNTs) and boron nitride nanotubes (BNNTs) were added to ca. 4mL of 100µM surfactant (E10 for BNNTs, R10 for CNTs) in water at an initial concentration of 0.125mg/mL. The mixture was bath ultrasonicated for 10 minutes (Cole-Parmer 8891, 42 kHz). The resulting dispersion was diluted by half with water and then 0.5µL was applied to a glass slide and allowed to dry. After drying, 100µL of water was added to the slide, to remove some excess surfactant, and blotted with a Kim Wipe. Slides were imaged using a Zeiss Axiovert 200M epi-fluorescence microscope with a TRITC filter cube (Chroma; λ_{ex} 527-552/ 565 dichroic/ λ_{em} 577-632 nm), a 100x oil immersion objective (N.A.=1.3), and a Toupcam industrial digital camera with a 1.4MP Sony CCD sensor, controlled by ToupView software.

4 Results & Discussion

Eight fluorescent surfactants (Fig. 1) were synthesized through an esterification reaction between two fluorescent dyes (Rhodamine B and Eosin Y) and alcohols with carbon chains of varying lengths (6, 10, 12, and 16 carbons). Initial synthetic attempts, using a standard Fisher esterification, yielded too many biproducts that were difficult to separate. We, therefore, decided to try a milder reaction based on the Garegg-Samuelsson reaction.[25] This reaction proceeds through the formation of an alkoxyphosphonium intermediate that is then attacked by the alcohol to generate the desired ester. The reaction scheme and resulting % yields for the reaction are listed in Table 1. Our yields are lower than what has been typically reported for the reaction of aliphatic carboxylic acids with small alcohols, however, it is important to note that

our carboxylic acid is in the ortho position of a benzyl group, (Fig. 1) where there can be significant steric constraints, leading to lower yields.

Table 1. Reaction scheme and percent yields for the eight surfactants studied.

[Insert file: Rxn Scheme.jpg]

Sample	Dye	Alcohol	% Yield
R6	Rhodamine B	Hexanol	20.9%
R10		Decanol	12.4%
R12		Dodecanol	25.1%
R16		Hexadecanol	7.6%
E6	Eosin Y	Hexanol	12.1%
E10		Decanol	8.7%
E12		Dodecanol	8.9%
E16		Hexadecanol	14.4%

The resulting surfactants form visible bubbles when shaken, consistent with the formation of micelles, and present intense fluorescence (Fig. 2). To characterize these behaviors, the surfactants were analyzed by determining their critical micelle concentration (CMC) and their fluorescence properties. As Rhodamine B produces positively charged surfactants and Eosin Y produces negatively charged surfactants, the eight surfactants could be compared based on charge and aliphatic chain length.

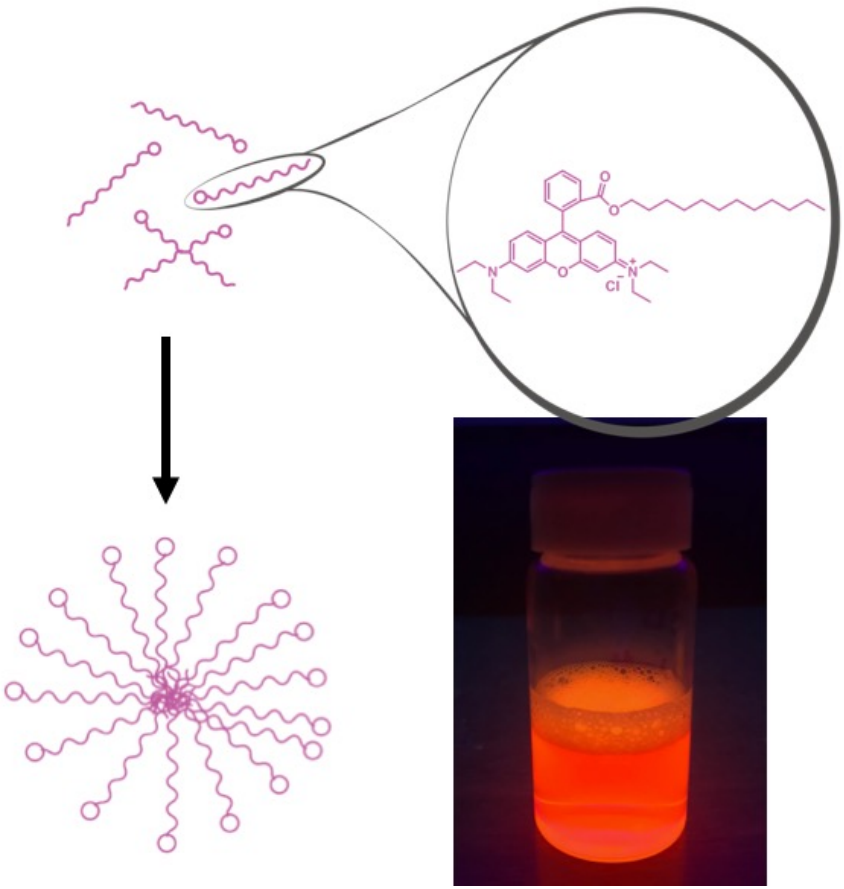

Fig. 2: Schematic demonstrating formation of micelle from surfactant molecules and picture of surfactant (R12) solution with bubble formation and intense fluorescence.

When surfactants are added to an aqueous solution at low concentrations, they remain free in solution and act similarly to any electrolyte, decreasing the surface and interfacial tension of the solution.[1,2] However, above a certain concentration (the CMC), the surfactant will aggregate to form micelles.[1-4] The CMC was determined for all eight surfactants (Fig. 3) by measuring the interfacial tension with increasing concentration, utilizing the pendant drop method.[26] Briefly, a drop of solution with a known concentration of surfactant is imaged as it hangs from the tip of a syringe – forming a 'pendant' shape. The drop shape is analyzed to calculate interfacial tension between the solution and surrounding air. As surfactant concentration increases, the

interfacial tension will slowly decrease until reaching a plateau. The point at which the change in interfacial tension levels off is the CMC (Fig. 3b, ESI). The measured CMC values for the Rhodamine B surfactants were 2.4 mM (R6), 1.2 mM (R10), 0.75 mM (R12), and 0.65 mM (R16), and for the Eosin Y surfactants were 3 mM (E6), 2.3 mM (E10), 1.4 mM (E12), and 1.1 mM (E16).

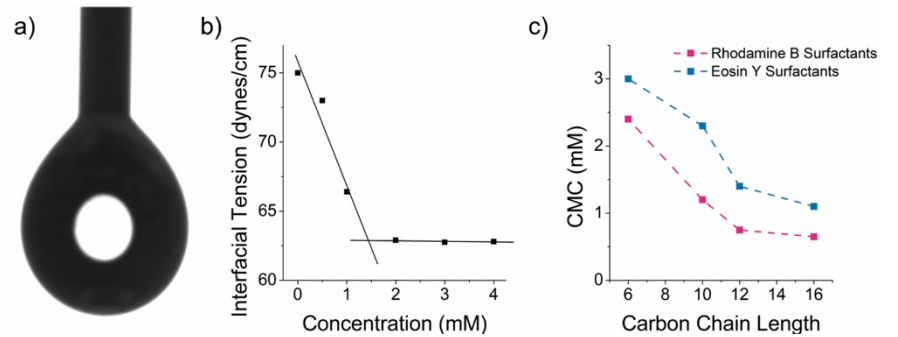

Fig. 3: Example pendant drop image (a) and interfacial tension measurements (b) for surfactant E12. Trends in CMC for the eight surfactants as a function of aliphatic chain length in number of carbons (c). The Rhodamine surfactants (pink) have CMCs of 2.4 mM (R6), 1.2 mM (R10), 0.75 mM (R12), and 0.65 mM (R16), while the Eosin surfactants (blue) have CMCs of 3 mM (E6), 2.3 mM (E10), 1.4 mM (E12), and 1.1 mM (E16).

The eight surfactants show a decrease in CMC with increasing aliphatic chain length, as expected from published CMCs for common surfactants.[3] The longer the carbon chain gets, the more hydrophobic the surfactant becomes, promoting micelle formation at lower concentrations. A similar trend is seen when comparing sodium alkyl sulfate surfactants of varying alkyl chain lengths. Sodium hexadecyl sulfate has a CMC of 0.5 mM, which increases to 8 mM, 33 mM, and 4.6 M when the alkyl group is changed to dodecyl, decyl, and hexyl respectively.[3] The change in CMC with decreasing aliphatic chain length is not as dramatic in our surfactants, likely due to intermolecular interactions, such as π-π stacking, between the dye molecules further promoting molecular association at lower concentrations. This observation is supported by the CMC values for sodium alkyl benzene sulfonate surfactants. Sodium hexadecyl benzene sulfonate has a CMC of 0.5 mM, which increases to 1.19 mM, 3.7 mM, and 37 mM with the switch in alkyl group to dodecyl, decyl and hexyl respectively.[3] As the fluorescent surfactants reported here contain even more conjugation

for π-π stacking interactions to occur, it is understandable why the change in CMC with decreasing carbon chain length is even further diminished. Finally, the four Eosin surfactants have slightly larger CMC values, for all aliphatic chain lengths, than the Rhodamine surfactants. This cannot be accounted for with charge, as common ionic surfactants with the same aliphatic chain length, sodium alkyl sulfate and alkyl ammonium chloride, show the opposite trend: the anionic, sodium alkyl sulfate surfactants demonstrate a smaller CMC than the cationic, ammonium alkyl chloride surfactants.[3] However, focusing more closely on the dyes' structures elucidates the reason for this difference. Eosin Y contains four Br groups around the xanthene core. As Br groups are very bulky, these additions most likely disrupt some of the π-π interactions between Eosin groups, slightly impeding micelle formation.

In addition to studying micelle formation of each surfactant, we also investigated the photoluminescence properties of the surfactants through fluorescence studies. Fig. 4 (a & c) show normalized UV-visible absorbance and emission spectra for the Rhodamine (4a) and Eosin (4c) surfactants. Changing the aliphatic chain length of the surfactant did not impact these spectra, so only the R6 and E6 spectra are shown. The fluorescence quantum yield (ϕ) of each surfactant (Fig. 4 b & d) was calculated using the equation $\phi_X = \phi_{ST}(Grad_X/Grad_{ST})$ where X and ST denote the sample and standard, respectively, and Grad refers to the slope of the plot of integrated photoluminescence as a function of absorbance. Rhodamine B (ϕ_{ST} = 0.31)[28] was used as the standard in all cases.

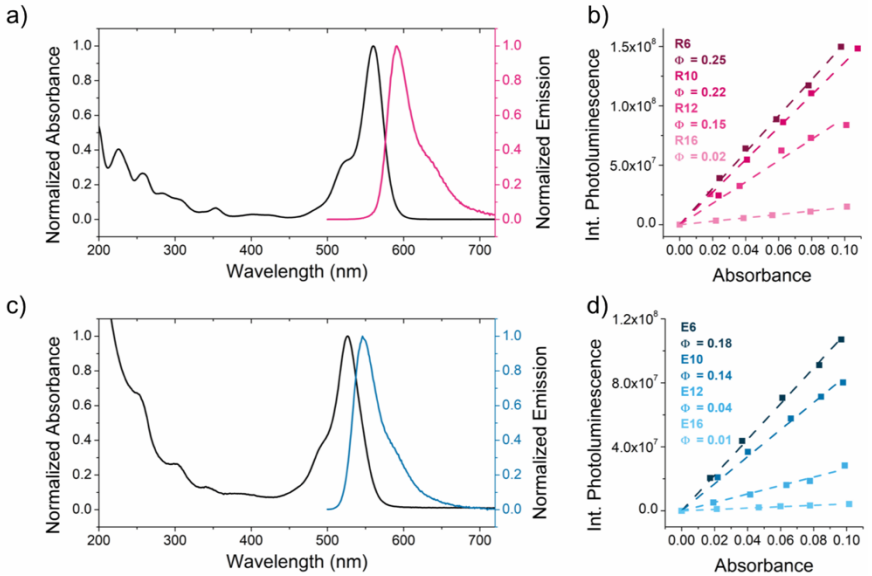

Fig. 4: Absorbance and emission spectra for R6 (a) and E6 (c) surfactants. These spectra did not change with different aliphatic chain lengths. Quantum yield measurements for Rhodamine (b) and Eosin (d) surfactants show a decrease in quantum yield with increasing aliphatic chain length. The Rhodamine surfactants had quantum yields of 0.25 (R6), 0.22 (R10), 0.15 (R12), and 0.02 (R16), and the Eosin surfactants had quantum yields of 0.18 (E6), 0.14 (E10), 0.04 (E12), and 0.01 (E16).

Quantum yield measurements show that increasing the aliphatic chain length leads to quenching of the fluorescence (Fig. 4 b & d). While the 6-carbon chain surfactants had quantum yields similar to those of their parent dye (ϕ_{RB} = 0.31, ϕ_{R6} = 0.25, ϕ_{EY} = 0.20, ϕ_{E6} = 0.18), the quantum yield decreased with increasing chain length (ϕ_{R10} = 0.22, ϕ_{R12} = 0.15, ϕ_{R16} = 0.02; ϕ_{E10} = 0.14, ϕ_{E12} = 0.04, ϕ_{E16} = 0.01). This further supports that the dye molecules are interacting through π-π stacking interactions, as these interactions can promote deactivation by nonradiative pathways, and thus quench the emission. Such quenching was previously reported by Enoki and Katoh in aggregates of Eosin Y.[29] Although all measurements were performed well below the CMC of the surfactants, associations can happen between these molecules, which will be more favorable the more hydrophobic they become. In addition, quenching could also occur through interaction of the dye with the aliphatic chain that

will likely wrap around the aromatic dye in order to reduce contact with water molecules. To further investigate this result, the quantum yields of R12 and E12 were additionally tested in 1 wt. % CTAC (~31 mM) and SDS (~35 mM), respectively. These concentrations were well above the surfactants' CMCs (1.3 mM for CTAC and 8 mM for SDS) [3]. This was expected to produce mixed micelles which could prevent aggregation of the dye and, therefore, increase its quantum yield. As expected, the quantum yields of the two surfactants increased in this environment from ϕ_{R12} = 0.15 and ϕ_{E12} = 0.04 to ϕ_{R12} = 0.25 and ϕ_{E12} = 0.16.

Throughout this manuscript we have proven the amphiphilic Rhodamine-B and Eosin Y act as surfactants, and have characterized their spectral properties. These surfactants could be utilized in a variety of applications, such as industrial and research purposes, depending on the surfactant properties required. Here we demonstrate that fluorescent surfactants can be used as tools for cellular and nanomaterial imaging. Cellular membranes are similar to surfactants, in that they are composed of amphiphilic molecules (phospholipids) that orient in a bilayer so that the hydrophilic phosphate heads interact with the aqueous surroundings and shield the hydrophobic tails in the interior. Therefore, it is logical that a surfactant molecule, as long as it is kept below its CMC, could simply insert itself within the membrane. In addition to the cellular membrane, most organelles, such as the mitochondria, endoplasmic reticulum, and lysosomes, are also enveloped in a membrane bilayer. Confocal images of Panc-1 cells incubated with R16 (500 nM in PBS) show a granular diffuse staining of the cell (Fig. 5), which is likely produced by binding organelle membranes. These studies show that fluorescent surfactants can be utilized as a novel full cell stain.

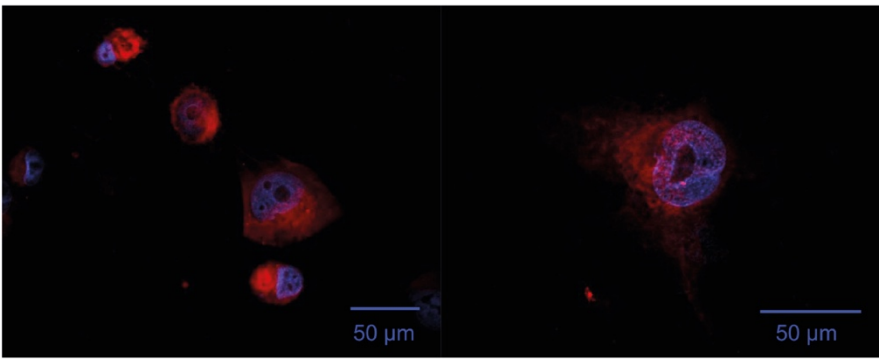

Fig. 5: Confocal microscope images of Panc-1 cells incubated with R16 (500 nm in PBS). (a) 40x magnified image of 4 cells shows the R16 surfactant enters the cell but

remains outside the nucleus. (b) 60x magnified compressed z-stack image of a single cell reveals pockets in the R16 staining that could be produced by the dye's localization in organelle membranes.

Another application for these surfactants is in the dispersion and imaging of nanomaterials. Surfactants are commonly used for nanomaterial dispersion[30-32] as these materials are typically hydrophobic in nature. In the case of carbon and boron nitride nanotubes, utilizing surfactants has been shown to produce individualized nanotubes well dispersed in aqueous solution.[30,31] With a fluorescent surfactant, these individualized tubes can then be imaged using standard fluorescence microscopy. In figure 6 we demonstrate this with CNTs (Fig. 6A) and BNNTs (Fig. 6B) immobilized on a glass slide. The individualized nanotubes can be easily visualized and studied with minimal sample preparation.

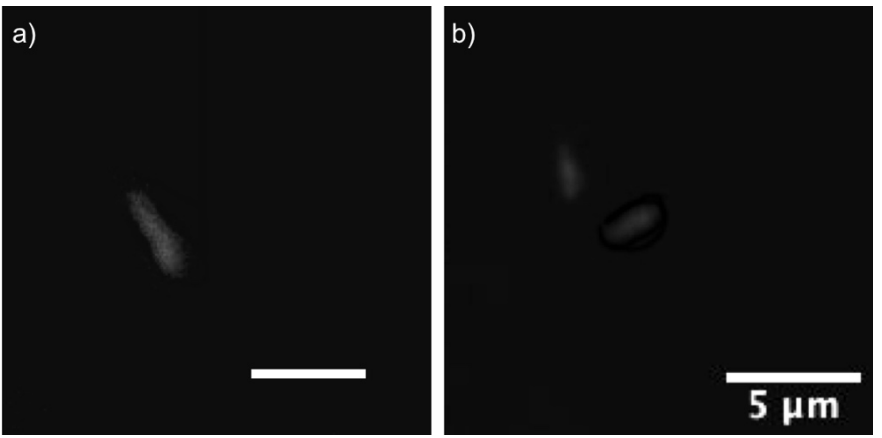

Fig. 6: Fluorescence microscope images of individual CNT (a) and BNNTs (b) dispersed in the fluorescent surfactants R10 and E10, respectively, and drop casted onto a glass microscope slide.

5 Conclusion

Eight fluorescent surfactants were synthesized by an esterification reaction between a fluorescent dye (Rhodamine B or Eosin Y) and an alcohol (hexanol, decanol, dodecanol, or hexadecanol). The CMC and fluorescence properties were studied for each surfactant. The CMC increased with decreasing aliphatic chain length, but not to

the same degree as is seen with sodium alkyl sulfate surfactants, suggesting that intermolecular interactions between the dye molecules promotes micelle formation. The fluorescence quantum yield also decreases with increasing aliphatic chain length, which is consistent with increased intermolecular interactions. Finally, we show the full cellular staining and imaging using the fluorescent surfactant, R16. As well as, the dispersion and imaging of CNTs and BNNTs using the fluorescent surfactants R10 and E10, respectively. Surfactants are widely utilized compounds in a vast array of applications, from detergents to industrial foams. Adding fluorescence capabilities to surfactants extends their potential applications and makes some processes more efficient that typically require both surfactants and dyes to perform. Our modular approach to surfactant synthesis will allow for further production of a full line of fluorescent surfactants with varied photoluminescence and surface properties.

6 Acknowledgments

We acknowledge the NSF (CHE 1807737) for financial support.

7 References

(1) L. L. Schramm, E. N. Stasiuk, D. G. Marangoni. Annu. Rep. Prog. Chem., Sect. C Phys. Chem. 99, 3 (2003).
(2) M. J. Rosen, J. T. Kunjappu. Surfactants and Interfacial Phenomena, pp. 1-9, John Wiley & Sons, Inc., Hoboken, New Jersey (2012).
(3) P. Mukerjee, K. J. Mysels. Critical Micelle Concentrations of Aqueous Surfactant Systems. 36 (1971).
(4) A. Dominguez, A. Fernandez, N. Gonzalez, E. Iglesias, L. Montenegro. J. Chem. Educ. 74, 1227 (1997).
(5) I. Kralova, J. Sjöblom. J. Dispers. Sci. Technol. 30, 1363 (2009).
(6) M. A. Migahed, A. M. Al-Sabagh. Chem. Eng. Commun. 196, 1054 (2009).
(7) A. C. Hellgren, P. Weissenborn, K. Holmberg. Prog. Org. Coatings. 35, 79 (1999).
(8) S. Baliarsingh, J. Jena, T. Das, N. B. Das. Ind. Crops Prod. 50, 618 (2013).
(9) R. Duggal, M. Pasquali. Phys. Rev. Lett. 96, 246104 (2006).
(10) R. Prakash, S. Washburn, R. Superfine, R. E. Cheney, M. R. Falvo. Cit. Appl. Phys. Lett. 83, 1219 (2003).
(11) J. Niskanen, I. Zhang, Y. Xue, D. Golberg, D. Maysinger, F. M. Winnik. Nanomedicine (Lond.). 11, 447 (2016).
(12) P. J. Bennion, R. W. Horobin, L. B. Murgatroyd. Stain Technol. 50, 307 (1975).
(13) Z. Xu, P. Li, W. Qiao, Z. Li, L. Cheng. Colloids Surf A. 290, 172 (2006).
(14) J. Wang, Z. Xu, Y. Zhao, W. Qiao, Z. Li. Dyes Pigm. 74, 103 (2007).

(15) P. Yin, P. Wu, Z. Xiao, D. Li, E. Bitterlich, J. Zhang, P. Cheng, D. V. Vezenov, T. Liu, Y. Wei. Angew. Chem. Int. Ed. 50, 2521 (2011).
(16) D. J. Boday, J. Kuezynski, J. T. Wertz, J. Zhang. US Patent 2014/0145094 A1, Filed 29 Nov 2012, Issued 29 May 2014.
(17) J. A. Ross, B. P. Ross, K. L. Cosgrove, H. Rubinsztein-Dunlop, R. P. McGeary. Molbank. 2006, M515 (2006).
(18) B. Yu, C. Y. Dong, P. T. C. So, D. Blankschtein, R. Langer. Proc. SPIE. 4262, 217 (2001).
(19) T. I. Rokitskaya, G. A. Korshunova, Y. N. Antonenko. Biophys. J. 115, 514 (2018).
(20) T. Matsumura, K. Hirabayash. US Patent 2004/0091816 A1, Filed 17 Oct 2003, Issued 13 May 2004.
(21) B. M. Estevão, D. S. Pellosi, C. F. de Freitas, D. Vanzin, D. S. Franciscato, W. Caetano, N. Hioka. J. Photochem. Photobiol. A. 287, 30 (2014).
(22) S. Troppmann, B. König. Chem. Eur. J. 20, 14570 (2014).

(23) F. Liang, A. K. Sadana, A. Peera, J. Chattopadhyay, Z. Gu, R. H. Hauge, W. E. Billups. Nano Lett. 4, 1257 (2004).
(24) H. Chen, Y. Chen, J. Yu, J. S. Williams. Chem. Phys. Lett. 425, 315 (2006).
(25) S. P. Morcillo, L. Álvarez de Cienfuegos, A. J. Mota, J. Justicia, R. Robles. J. Org. Chem. 76, 2277 (2011).
(26) E. Y. Arashiro, N. R. Demarquette. Mater. Res. 2, 23 (1999).
(27) A. Daerr, A. Mogne. J. Open Res. Softw. 4, 3 (2016).
(28) D. Magde, G. E. Rojas, P. G. Seybold. Photochem. Photobiol. 70, 737 (1999).
(29) M. Enoki, R. Katoh. Photochem. Photobiol. Sci. 17, 793 (2018).
(30) V. C. Moore, M. S. Strano, E. H. Haroz, R. H. Hauge, R. E. Smalley. Nano Lett. 3, 1379 (2003).
(31) A. D. S. McWilliams, C. A. de los Reyes, L. Liberman, S. Ergülen, Y. Talmon, M. Pasquali, A. A. Martí. Nanoscale Adv. (2019). DOI: 10.1039/c8na00315g.
(32) R. J. Smith, M. Lotya, J. N. Coleman. New. J. Phys. 12, 125008 (2010).